# Abnormal findings on multiparametric prostate magnetic resonance imaging predict subsequent biopsy upgrade in patients with low risk prostate cancer managed with active surveillance

**Robert R. Flavell**, **Antonio C. Westphalen**, **Carmin Liang**, **Christopher C. Sotto**, **Susan M. Noworolski**, **Daniel B. Vigneron**, **Zhen J. Wang**, and **John Kurhanewicz**

Department of Radiology and Biomedical Imaging, University of California, San Francisco, 505 Parnassus Avenue, M-372, Box 0628, San Francisco, CA, USA

## Abstract

**Purpose**—To determine the ability of multiparametric MR imaging to predict disease progression in patients with prostate cancer managed by active surveillance.

**Methods**—Sixty-four men with biopsy-proven prostate cancer managed by active surveillance were included in this HIPPA compliant, IRB approved study. We reviewed baseline MR imaging scans for the presence of a suspicious findings on T2-weighted imaging, MR spectroscopic imaging (MRSI), and diffusion-weighted MR imaging (DWI). The Gleason grades at subsequent biopsy were recorded. A Cox proportional hazard model was used to determine the predictive value of MR imaging for Gleason grades, and the model performance was described using Harrell's C concordance statistic and 95% confidence intervals (CIs).

**Results**—The Cox model that incorporated T2-weighted MR imaging, DWI, and MRSI showed that only T2-weighted MR imaging and DWI are independent predictors of biopsy upgrade (T2; HR = 2.46; 95% CI 1.36–4.46; $P = 0.003$—diffusion; HR = 2.76; 95% CI 1.13–6.71; $P = 0.03$; $c$ statistic = 67.7%; 95% CI 61.1–74.3). There was an increasing rate of Gleason score upgrade with a greater number of concordant findings on multiple MR sequences (HR = 2.49; 95% CI 1.72–3.62; $P < 0.001$).

**Conclusions**—Abnormal results on multiparametric prostate MRI confer an increased risk for Gleason score upgrade at subsequent biopsy in men with localized prostate cancer managed by active surveillance. These results may be of help in appropriately selecting candidates for active surveillance.

## Keywords

Prostate cancer; Active surveillance; Magnetic resonance imaging; Magnetic resonance spectroscopic imaging; Diffusion-weighted magnetic resonance imaging

Prostate cancer is the most prevalent noncutaneous cancer in men, and presents with a broad clinical spectrum ranging from indolent to rapidly progressive disease. Due to the complications of definitive treatment with either surgery or radiation, active surveillance has emerged as a management strategy for patients with low risk prostate cancer. In this protocol, patients are followed with serial PSA measurements, clinical exam, and biopsy, with the aim of avoiding or delaying definitive treatment [1]. However, a subset of patients managed on active surveillance develop worsening cancer, manifested by increase in Gleason score or increased volume of disease on subsequent biopsy, and therefore may require definitive treatment [2, 3].

Multiparametric magnetic resonance (MR) imaging is a promising tool for predicting which patients will progress on subsequent biopsy, and therefore fail active surveillance. While MR imaging protocols vary from practice to practice, all include T2-weighted MR imaging. Other sequences that are used are diffusion-weighted MR imaging (DWI), magnetic resonance spectroscopic imaging (MRSI), and dynamic contrast-enhanced MR imaging (DCE) [4–7]. The role of MR imaging in the management of patients on active surveillance is controversial; however, prior studies have demonstrated a correlation between abnormal MR imaging findings and high-grade cancer [8–10].

Accordingly, the goal of this study was to determine the ability of multiparametric MR imaging to predict disease progression in patients with prostate cancer managed by active surveillance.

## Materials and methods

### Subjects and outcome

Our institutional review board approved this retrospective cohort study. Informed consent was prospectively obtained from all study participants at the time of scanning and before their data were entered into our HIPAA compliant database for use in future research. A single author (CL) searched our database for all MR imaging scans done prior to June 30th, 2012, and collected patients' clinical data. The electronic medical record of all patients was reviewed.

Inclusion criteria were as follows:

– Biopsy-proven prostate cancer managed with active surveillance at our institution.

– Gleason score 6 or less, without grade 4 or 5.

– Total serum PSA 10 ng/mL.

– Clinical stage T2B.

– Multiparametric MR imaging done within 18 months of the diagnosis. We opted for this time interval because in our institution patients under active surveillance undergo PSA follow-up every 3–4 months and MR imaging and/or TRUS-guided biopsy between 6 and 18 months.

– Follow-up transrectal ultrasound-guided biopsy of the prostate. Some patients had multiple subsequent biopsies.

Patients in which any one of the MR imaging sequences was non-diagnostic were excluded from the study.

The outcome of interest was disease progression under active surveillance, which was characterized as Gleason score upgrade, i.e., identification of Gleason grade 4 or 5 at any subsequent biopsy. Our institution's current TRUS-guided biopsy protocol acquires 12–14 core specimens systematically, cores targeted to any sonographic abnormality, and cores targeted to findings seen on MR imaging, when applicable. The time to most recent biopsy or disease progression was recorded.

## MR imaging technique

MR studies were performed with a 1.5 T (Signa; GE Healthcare, Waukeshaw, WI) or a 3.0 T (GE Healthcare Technologies, Waukeshaw, WI) whole-body MR scanner. Patients were imaged in a supine position. A body coil was used for excitation, and a pelvic phased-array coil (GE Healthcare, Waukeshaw, WI) and a commercially available expandable balloon endorectal coil (Medrad, Pittsburg, PA) filled with perfluorocarbon (Flutech_T14 TM, F2 Chemicals, UK) were used for signal reception. After a 3D localizer scan, axial and coronal T2-weighted high spatial resolution fast spinecho magnetic resonance (MR) images (3 mm/0 mm, TR/TE = 6000/96 ms, ETL-16, FOV-14, $256 \times 256$) of the prostate and seminal vesicles were acquired to identify prostate zonal anatomy and pathology. Axial spinecho T1-weighted MR images (5 mm/1 mm, TR/ TE = 9/950 ms, FOV-24, $256 \times 256$) were obtained from the aortic bifurcation to the symphysis pubis for the assessment of pelvic lymph node and bone metastases. Diffusion-weighted MR images (DWI) were acquired using either a 2D single-shot fast spin echo (SSFSE)-DWI sequence or a 2D single-shot EPI spin-echo DWI sequence. The DWI images were obtained with slice locations and obliquity identical to the oblique axial T2-weighted images. The SSFSE-DWI images were acquired with the following parameters: FOV = 24 cm, $256 \times 128$, slice thickness = 3 mm, 62 kHz bandwidth, $b = 0 + 600$, 6-gradient directions, single-shot (sub-second), with four repetitions. The EPI-DWI images were acquired with the following parameters: FOV = 24 cm, $256 \times 128$, slice thickness = 3 mm, 200 kHz bandwidth, $b = 0 + 600$, six-gradient directions, single-shot (subsecond), with four repetitions. At both 1.5 and 3 T, 3D MR spectroscopic imaging (MRSI) data were acquired using a water- and lipid-suppressed double-spin-echo point resolved spectroscopy sequence with spectral-spatial pulses for the two 180° excitation pulses, and outer-voxel saturation pulses. Using this sequence at 1.5 T, 0.24 cc resolution MRSI data were acquired with; NEX = 1, $16 \times 8 \times 8$ phase encoding, and a TR/TE = 1000/130 ms, yielding a scan time of 8 min. Using a MLEV-PRESS sequence [11] at 3 T, 0.24 cc resolution MRSI data were acquired with; NEX = 1, $16 \times 10 \times 8$ phase encoding using an interleaved echo-planar spectroscopic readout in the left–right dimension, TR/ TE = 2000/85 ms, yielding a scan time of 8 min. The total exam time including patient setup and acquisition of the MR data was approximately 1 h.

## Image interpretation

Imaging findings on all three modalities were determined for each half of the gland. All three imaging parameters were reviewed independently, without comparison with other imaging sequences. Except for the fact that patients had prostate cancer, readers were unaware of clinical and histological data during imaging assessment.

T2-weighted MR images were jointly analyzed by RF and AW, radiologists with 2-and 15-year experience, respectively. A five-point scale based on the approach proposed by Barentsz et al. [12] was used to characterize each half of the gland (1 = definitely no cancer; 2 = probably no cancer; 3 = indeterminate; 4 = probably cancer; 5 = definite cancer). A score of 4 or 5 was considered as a positive result.

DWI were analyzed using apparent diffusion coefficient (ADC) maps. Diffusion-weighted imaging was scored in a binary way; an abnormal scan was characterized by the presence of a region of low signal intensity, with volume greater than 0.03 cc, which contained ADC values lower than the threshold value indicative of significant cancer. Regions of interest (ROIs) were drawn by two authors, AW and RF, on the ADC maps on all suspicious foci, and the mean ADC values were obtained. For images acquired with the echo-planar imaging sequence, the threshold was $1100 \times 10^{-6}$ mm$^2$/s. The ADC threshold for prostate cancer was empirically determined to be 18% lower using the Fast Spin Echo (FSE) sequence which was similar to a previously published values [13]. In addition, recent studies have correlated the ADC values obtained at MR imaging with radical prostatectomy specimens, with mean values ranging from 860 to $1100 \times 10^{-6}$ mm$^2$/s indicative of the presence of Gleason 4 pattern tumor [14–18]. Accordingly, a value of $900 \times 10^{-6}$ mm$^2$/s was computed for the cancer threshold for the SSFSE DWI studies. There is known variation of ADC values up to 5% at different field strengths, based on phantom studies [19]. To our knowledge, however, this phenomenon has not been investigated in prostate MR imaging. Therefore, we opted for not normalizing ADC values for field strength.

MR spectroscopic imaging was scored in a binary way, with a positive MR spectroscopic imaging defined as an exam with three or more consecutive voxels having a choline + creatine to citrate (CC/C) ratio   3 standard deviations above the mean healthy peripheral zone value. The use of standard deviations to categorize MR spectroscopic findings is one of the recommended interpretative approaches proposed by Barentsz et al. [12]; a CC/ C ratio   3 standard deviations represents scores 4 and 5 in that publication. For exams performed with a 1.5 T magnet, the normal mean CC/C ratio was empirically determined to be $0.26 \pm 0.13$ which was close to the previously published value [20]. On a 3.0 T scanner, the normal mean CC/C ratio was empirically determined to be $0.43 \pm 0.18$. MR spectroscopic images were data were processed off-line on an UltraSparc workstation (Sun Microsystems, Mountain View, CA) utilizing in-house software previously developed specifically for 3D-MR spectroscopic imaging studies. Integrated peak area values for choline, creatine, and citrate and peak area ratios for choline to creatine and choline plus creatine to citrate were automatically calculated for each voxel. This process was performed by a medical MR spectroscopist, JK, who has 23 years of experience on spectroscopic imaging. Images were then jointly reviewed by RF and AW for analysis.

In addition, we classified patients into groups based on the number of positive imaging parameters: (a) men with normal examinations, (b) men with one positive MR sequence, (c) men with any two concordant positive MR imaging sequences, and (d) men with concordant positive findings on all three MR sequences.

## Statistical analyses

Median and range were used to describe the patient cohort with respect to clinical, imaging, and outcome variables. Cox proportional hazard models were used to determine the probabilities of biopsy upgrade at subsequent TRUS-guided biopsy (Gleason score upgrade, defined as identification of Gleason grade 4 or 5, on subsequent biopsy). As MR imaging abnormalities were localized to the right or left hemiprostate, the analyses were performed taking into account the cluster effect, therefore allowing for the calculation of robust standard errors. The Cox models were built with (1) a single predictor (T2-weighted MRI results, diffusion-weighted MRI results, or MRSI results); and (2) all three predictors (T2-weighted MRI results, diffusion-weighted MRI results, and MRSI results) to estimate the probability of a positive outcome. The performance of each diagnostic approach was described using Harrell's C concordance statistic and 95% confidence intervals (CIs). The *c* statistic measures how well the model predicts the outcome and is analogous to the area under the receiver-operating characteristic curve.

Fisher's exact test was be used to assess whether men with a greater number of positive MR parameters (all negative, only one, any two, or all three positive sequences, i.e., T2-weighted MR imaging, diffusion-weighted MR imaging, and MR spectroscopic imaging) were more likely to present Gleason upgrade on a subsequent biopsy. An additional secondary univariate survival analysis was performed using the number of positive parameters as a predictor of biopsy upgrade.

Statistical calculations were performed using Stata 13.1 (College Station, TX). All test was two-tailed and a 5% level of confidence was considered significant.

## Results

### Subjects and outcome

A total of 69 men were eligible for the study, but five were excluded due to non-diagnostic images (diffusionweighted MR imaging = 1; MR spectroscopic imaging = 2; both = 2). Our final study population was composed of 64 men with a median age of 60.7 years (range 45.1–74.5). The median total serum PSA was 4.7 ng/ml (range 0.6–9.7). All men had a Gleason score of 3 + 3 at baseline. Most men (51/64, 80%) presented with clinical stage T1C (no palpable abnormality of digital rectal examination). Of the 64 patients, 33 (52%) showed Gleason upgrade on a subsequent biopsy. These and other characteristics are summarized in Table 1.

### MR imaging

Forty-three scans (67%) were performed on a 1.5 T magnet, while 21 (33%) were done on a 3.0 T magnet. Imaging was positive on T2-weighted MR imaging in 35 patients (35/64,

55%); in 12 men (12/64, 19%) findings were bilateral. On MR spectroscopic imaging, 19 men (19/64, 30%) demonstrated positive results, i.e., 3 or more contiguous abnormal voxels. Findings were bilateral in six patients (6/64, 9%). Diffusion-weighted MR imaging was obtained using echo-planar imaging (23/64, 36%), fast spin echo (41/64, 64%) sequences. Fourteen patients (14/64, 22%) demonstrated positive findings on ADC maps, in two of which it was bilateral (2/64, 3%). These results are summarized in Table 2. One representative normal examination and one representative examination with a concordant T2-weighted MR imaging, diffusion-weighted MR imaging, and MR spectroscopic imaging abnormalities are presented in Figures 1 and 2.

### Outcome prediction

Using univariate analyses, all three imaging parameters predicted failure of active surveillance, with hazard ratios of 3.07 (95% CI 1.81–5.21; $P < 0.001$) for T2-weighted MR imaging, 5.25 (95% CI 2.79–9.86; $P < 0.001$) for DWI, and 2.26 (95% confidence interval 1.21–4.23; $P = 0.01$) for MRSI.

The Cox proportional hazard model that incorporated all imaging parameters (T2-weighted MR imaging, DWI, and MRSI) showed that only T2-weighted MR imaging and diffusion-weighted MR imaging remained as independent predictors of biopsy upgrade in a statistically significant manner (T2; hazard ratio = 2.46; 95% CI 1.36–4.46; $P = 0.003$—diffusion; hazard ratio = 2.76; 95% CI 1.13–6.71; $P = 0.03$). The $c$ statistic for this model was 67.7% (95% CI 61.1–74.3).

Table 3 shows that an increasing rate of Gleason score upgrade was seen with a greater number of concordant positive sequences ($P = 0.008$). Seven of twenty-five men with normal exams (28%) had subsequent biopsy upgrade, compared to 13/22 (59%) with one positive MR sequence, 3/5 (60%) with two positive MR sequences, and 10/12 (83%) of patients in whom all three sequences were positive. The survival analysis demonstrated a hazard ratio of 2.49 for disease progression (95% CI 1.72–3.62, $P < 0.001$). In other words, a man with one additional positive parameter who has not yet progressed by a certain time has more than twice the chance of showing progression at a later point in time compared with someone with one fewer positive MR parameter. Notably, of the patients with a concordant T2, MRSI, and ADC abnormality 10/12 progressed on subsequent biopsy (positive predictive value of 0.83).

## Discussion

We found that multiparametric MR imaging can be used to assess the risk of prostate cancer progression in men under active surveillance. In particular, we found that T2-weighted MR imaging and diffusion-weighted MR imaging are independent predictors of Gleason score upgrade on subsequent biopsies and that the probability of disease progression gets higher as the number of positive MR sequences of a multiparametric protocol increases.

Prior studies have aimed to characterize the role of prostate MR imaging in active surveillance using two main approaches. First, imaging findings have been correlated with pathologic results in patients who would have qualified for active surveillance, but instead

underwent radical prostatectomy. Most of these studies have demonstrated that suspicious findings on various MR imaging sequences and on multiparametric protocols [14, 16, 21–29] correlate with adverse histology. Second, imaging findings have been correlated with subsequent disease progression in actual or potential active surveillance patients by various metrics, including PSA velocity [30, 31], progression to radical treatment [31–34], upgrade at biopsy [31, 33–40], or a combination of these metrics [31]. The primary utility of MR imaging in these patients is thought to be the detection of lesions that are under sampled in a conventional transrectal ultrasound-guided prostate biopsy, particularly in the anterior gland [2, 35, 37, 41]. Recent studies have correlated findings on multiparametric MRI with biopsy results using methodology different from our own, for example utilizing dynamic contrast-enhanced imaging, or using size criteria to define suspicious lesions [35, 37–40].

Our data provide important complementary information to the prior research. First, not all of these previous studies have used multiparametric MR imaging [30, 32–34], which is now considered by many experts the current standard of care and has been supported by wellknown institutions in the field, including the European Society of Urogenital Radiology, the AdMeTech Foundation, and the American College of Radiology [42]. Also, in comparison with other recent reports that did investigate multiparametric MR imaging [37–40], our study includes post-MRI transrectal ultrasound-guided biopsy data on all patients, which is currently considered standard of care in active surveillance patients. In particular, some of these studies correlated imaging findings with patients who had already progressed, and therefore failed active surveillance, at the time of MRI [39, 40]. Other studies used MR-guided biopsy, which is a promising novel technique for detection of progression, but is still considered experimental [37], or only performed biopsies in patients with positive MR results [38]. Our study aims to answer a different question, namely whether an MRI predicts failure of active surveillance at a subsequent biopsy using otherwise standard of care methods.

Arguably, radical prostatectomy specimens would provide the optimal standard of reference to determine Gleason score upgrading, as TRUS-guided biopsy has well-known sampling limitations. Our option to use TRUS-guided biopsy has, therefore, led to more conservative results. If Gleason score upgrading was predicted on MR imaging, but not detected by TRUS-guided biopsy, we counted the result as a false-positive results of MR imaging. Yet, our results suggest MR imaging is a helpful tool to predict Gleason score upgrading, perhaps to a greater extent than described herein.

Our study has limitations. First, this was a single center study and our patient population that may not reflect the active surveillance population as a whole. In particular, programs for active surveillance have slightly different inclusion criteria at different institutions. For example, some institutions include patients with Gleason 3 + 4 disease, or exclude patients with T2 clinical stage disease. Yet, our results are, arguably, still applicable to this other population, as these men start active surveillance with a higher grade tumor. These variations limit the generalizability of single center studies such as our own. Additionally, the patient population in this study is 86% of Caucasian ethnicity, which may not reflect the distribution in other communities. Second, our study did not include DCE MR imaging, which is often included in multiparametric MR imaging protocols. It is possible that the

addition of DCE would have improved the predictive power of the multiparametric MRI, although no study has shown this to be the case in an active surveillance population to date. Third, our study used a heterogeneous technique, including MRI field strengths of 1.5 and 3 T, and three different diffusion-weighted sequences. Unfortunately, changing technology is a common problem for imaging outcomes studies since imaging technology is always improving over time. We attempted to minimize this problem by normalizing the data acquired at different field strengths and using slightly different acquisition protocols. While this normalization provides similar biomarker thresholds for identifying prostate cancer, it does not account for the improvement in data quality over time. Although this does present a complication, our aggregate data may in fact represent an average of what is performed in the radiology community at large and therefore may be more widely applicable. Finally, our study was retrospective in design, potentially leading to bias in patient selection. In particular, our study group had a high rate of progression on subsequent biopsy (52%) in comparison with other published series, suggesting there may have been a bias in selecting higher risk patients for MRI [3]. At least in part, this could also be explained by ''sampling bias'' at the time of the initial TRUS-guided prostate biopsy, rather than true progression. Irrespective, the results of our study demonstrate that MR imaging may be a good auxiliary tool to determine eligibility to active surveillance.

In conclusion, we found that abnormal results on multiparametric prostate MRI confer an increased risk for Gleason score upgrade at subsequent biopsy in men with localized prostate cancer managed by active surveillance. In particular, we found that the presence of concordant positive findings on T2, diffusion, and MR spectroscopic imaging had an 83% positive predictive value for progression at a subsequent biopsy. Additionally, only T2 and diffusion were independent predictors of biopsy upgrade. These results add to a growing body of literature that suggest that MR imaging may help predict which patients fail management by active surveillance.

# References

1. Dall'era MA, Albertsen PC, Bangma C, et al. Active surveillance for prostate cancer: a systematic review of the literature. Eur Urol. 2012; 62(6):976–983. [PubMed: 22698574]

2. Duffield AS, Lee TK, Miyamoto H, Carter HB, Epstein JI. Radical prostatectomy findings in patients in whom active surveillance of prostate cancer fails. J Urol. 2009; 182(5):2274–2278. [PubMed: 19758635]

3. Klotz L, Zhang L, Lam A, et al. Clinical results of long-term follow-up of a large, active surveillance cohort with localized prostate cancer. J Clin Oncol. 2010; 28(1):126–131. [PubMed: 19917860]

4. Yakar D, Debats OA, Bomers JG, et al. Predictive value of MRI in the localization, staging, volume estimation, assessment of aggressiveness, and guidance of radiotherapy and biopsies in prostate cancer. J Magn Reson Imaging. 2012; 35(1):20–31. [PubMed: 22174000]

5. Hoeks CM, Barentsz JO, Hambrock T, et al. Prostate cancer: multiparametric MR imaging for detection, localization, and staging. Radiology. 2011; 261(1):46–66. [PubMed: 21931141]

6. Hegde JV, Mulkern RV, Panych LP, et al. Multiparametric MRI of prostate cancer: an update on state-of-the-art techniques and their performance in detecting and localizing prostate cancer. J Magn Reson Imaging. 2013; 37(5):1035–1054. [PubMed: 23606141]

7. Bonekamp D, Jacobs MA, El-Khouli R, Stoianovici D, Macura KJ. Advancements in MR imaging of the prostate: from diagnosis to interventions. Radiographics. 2011; 31(3):677–703. [PubMed: 21571651]

8. Moore CM, Ridout A, Emberton M. The role of MRI in active surveillance of prostate cancer. Curr Opin Urol. 2013; 23(3):261–267. [PubMed: 23478498]

9. Ouzzane A, Puech P, Villers A. MRI and surveillance. Curr Opin Urol. 2012; 22(3):231–236. [PubMed: 22388665]

10. Dianat SS, Carter HB, Macura KJ. Performance of multiparametric magnetic resonance imaging in the evaluation and management of clinically low-risk prostate cancer. Urol Oncol. 2013

11. Chen AP, Cunningham CH, Kurhanewicz J, et al. High-resolution 3D MR spectroscopic imaging of the prostate at 3 T with the MLEV-PRESS sequence. Magn Reson Imaging. 2006; 24(7):825–832. [PubMed: 16916699]

12. Barentsz JO, Richenberg J, Clements R, et al. ESUR prostate MR guidelines 2012. Eur Radiol. 2012; 22(4):746–757. [PubMed: 22322308]

13. Kozlowski P, Chang SD, Goldenberg SL. Diffusion-weighted MRI in prostate cancer— comparison between single-shot fast spin echo and echo planar imaging sequences. Magn Reson Imaging. 2008; 26(1):72–76. [PubMed: 17566687]

14. Somford DM, Hambrock T, Hulsbergen-van de Kaa CA, et al. Initial experience with identifying high-grade prostate cancer using diffusion-weighted MR imaging (DWI) in patients with a Gleason score  3 + 3 = 6 upon schematic TRUS-guided biopsy: a radical prostatectomy correlated series. Investig Radiol. 2012; 47(3):153–158. [PubMed: 22293513]

15. Hambrock T, Somford DM, Huisman HJ, et al. Relationship between apparent diffusion coefficients at 3.0-T MR imaging and Gleason grade in peripheral zone prostate cancer. Radiology. 2011; 259(2):453–461. [PubMed: 21502392]

16. Itou Y, Nakanishi K, Narumi Y, Nishizawa Y, Tsukuma H. Clinical utility of apparent diffusion coefficient (ADC) values in patients with prostate cancer: can ADC values contribute to assess the aggressiveness of prostate cancer? J Magn Reson Imaging. 2011; 33(1):167–172. [PubMed: 21182135]

17. Verma SK, McClure K, Parker L, et al. Simple linear measurements of the normal liver: interobserver agreement and correlation with hepatic volume on MRI. Clin Radiol. 2010; 65(4): 315–318. [PubMed: 20338399]

18. Vargas HA, Akin O, Franiel T, et al. Diffusion-weighted endorectal MR imaging at 3 T for prostate cancer: tumor detection and assessment of aggressiveness. Radiology. 2011; 259(3):775–784. [PubMed: 21436085]

19. Chenevert TL, Galban CJ, Ivancevic MK, et al. Diffusion coefficient measurement using a temperature-controlled fluid for quality control in multicenter studies. J Magn Reson Imaging. 2011; 34(4):983–987. [PubMed: 21928310]

20. Males RG, Vigneron DB, Star-Lack J, et al. Clinical application of BASING and spectral/spatial water and lipid suppression pulses for prostate cancer staging and localization by in vivo 3D 1H magnetic resonance spectroscopic imaging. Magn Reson Med. 2000; 43(1):17–22. [PubMed: 10642727]

21. Lee DH, Koo KC, Lee SH, et al. Tumor lesion diameter on diffusion weighted magnetic resonance imaging could help predict insignificant prostate cancer in patients eligible for active surveillance: preliminary analysis. J Urol. 2013; 190(4):1213–1217. [PubMed: 23727188]

22. Puech P, Potiron E, Lemaitre L, et al. Dynamic contrast-enhanced- magnetic resonance imaging evaluation of intraprostatic prostate cancer: correlation with radical prostatectomy specimens. Urology. 2009; 74(5):1094–1099. [PubMed: 19773038]

23. Borofsky MS, Rosenkrantz AB, Abraham N, Jain R, Taneja SS. Does suspicion of prostate cancer on integrated T2 and diffusion-weighted MRI predict more adverse pathology on radical prostatectomy? Urology. 2013; 81(6):1279–1283. [PubMed: 23394882]

24. Nagarajan R, Margolis D, Raman S, et al. MR spectroscopic imaging and diffusion-weighted imaging of prostate cancer with Gleason scores. J Magn Reson Imaging. 2012; 36(3):697–703. [PubMed: 22581787]

25. Shukla-Dave A, Hricak H, Akin O, et al. Preoperative nomograms incorporating magnetic resonance imaging and spectroscopy for prediction of insignificant prostate cancer. BJU Int. 2012; 109(9):1315–1322. [PubMed: 21933336]

26. Park BH, Jeon HG, Choo SH, et al. Role of multiparametric 3.0 tesla magnetic resonance imaging in prostate cancer patients eligible for active surveillance. BJU Int. 2013

27. Turkbey B, Mani H, Aras O, et al. Prostate cancer: can multiparametric MR imaging help identify patients who are candidates for active surveillance? Radiology. 2013; 268(1):144–152. [PubMed: 23468576]

28. Guzzo TJ, Resnick MJ, Canter DJ, et al. Endorectal T2-weighted MRI does not differentiate between favorable and adverse pathologic features in men with prostate cancer who would qualify for active surveillance. Urol Oncol. 2012; 30(3):301–305. [PubMed: 21856187]

29. Ploussard G, Xylinas E, Durand X, et al. Magnetic resonance imaging does not improve the prediction of misclassification of prostate cancer patients eligible for active surveillance when the most stringent selection criteria are based on the saturation biopsy scheme. BJU Int. 2011; 108(4): 513–517. [PubMed: 21176083]

30. Cabrera AR, Coakley FV, Westphalen AC, et al. Prostate cancer: is inapparent tumor at endorectal MR and MR spectroscopic imaging a favorable prognostic finding in patients who select active surveillance? Radiology. 2008; 247(2):444–450. doi:247207077010.1148/radiol.2472070770. [PubMed: 18430877]

31. Fradet V, Kurhanewicz J, Cowan JE, et al. Prostate cancer managed with active surveillance: role of anatomic MR imaging and MR spectroscopic imaging. Radiology. 2010; 256(1):176–183. [PubMed: 20505068]

32. Morgan VA, Riches SF, Thomas K, et al. Diffusion-weighted magnetic resonance imaging for monitoring prostate cancer progression in patients managed by active surveillance. Br J Radiol. 2011; 84(997):31–37. [PubMed: 21172965]

33. Giles SL, Morgan VA, Riches SF, et al. Apparent diffusion coefficient as a predictive biomarker of prostate cancer progression: value of fast and slow diffusion components. AJR Am J Roentgenol. 2011; 196(3):586–591. [PubMed: 21343500]

34. van As NJ, de Souza NM, Riches SF, et al. A study of diffusion-weighted magnetic resonance imaging in men with untreated localised prostate cancer on active surveillance. Eur Urol. 2009; 56(6):981–987. [PubMed: 19095345]

35. Margel D, Yap SA, Lawrentschuk N, et al. Impact of multiparametric endorectal coil prostate magnetic resonance imaging on disease reclassification among active surveillance candidates: a prospective cohort study. J Urol. 2012; 187(4):1247–1252. [PubMed: 22335871]

36. Vargas HA, Akin O, Afaq A, et al. Magnetic resonance imaging for predicting prostate biopsy findings in patients considered for active surveillance of clinically low risk prostate cancer. J Urol. 2012; 188(5):1732–1738. [PubMed: 23017866]

37. Hoeks CM, Somford DM, van Oort IM, et al. Value of 3-T multiparametric magnetic resonance imaging and magnetic resonance- guided biopsy for early risk restratification in active surveillance of low-risk prostate cancer: a prospective multicenter cohort study. Invest Radiol. 2013

38. Stamatakis L, Siddiqui MM, Nix JW, et al. Accuracy of multiparametric magnetic resonance imaging in confirming eligibility for active surveillance for men with prostate cancer. Cancer. 2013; 119(18):3359–3366. [PubMed: 23821585]

39. Bonekamp D, Bonekamp S, Mullins JK, et al. Multiparametric magnetic resonance imaging characterization of prostate lesions in the active surveillance population: incremental value of magnetic resonance imaging for prediction of disease reclassification. J Comput Assist Tomogr. 2013; 37(6):948–956. [PubMed: 24270118]

40. Mullins JK, Bonekamp D, Landis P, et al. Multiparametric magnetic resonance imaging findings in men with low-risk prostate cancer followed using active surveillance. BJU Int. 2013; 111(7):1037–1045. [PubMed: 23464904]

41. Lawrentschuk N, Haider MA, Daljeet N, et al. 'Prostatic evasive anterior tumours': the role of magnetic resonance imaging. BJU Int. 2010; 105(9):1231–1236. [PubMed: 19817743]

42. International Scientific Cooperation to Advance Image-Guided Prostate Cancer Care. American College of Radiology News Releases. Reston: International Scientific Cooperation to Advance Image-Guided Prostate Cancer Care; 2012.
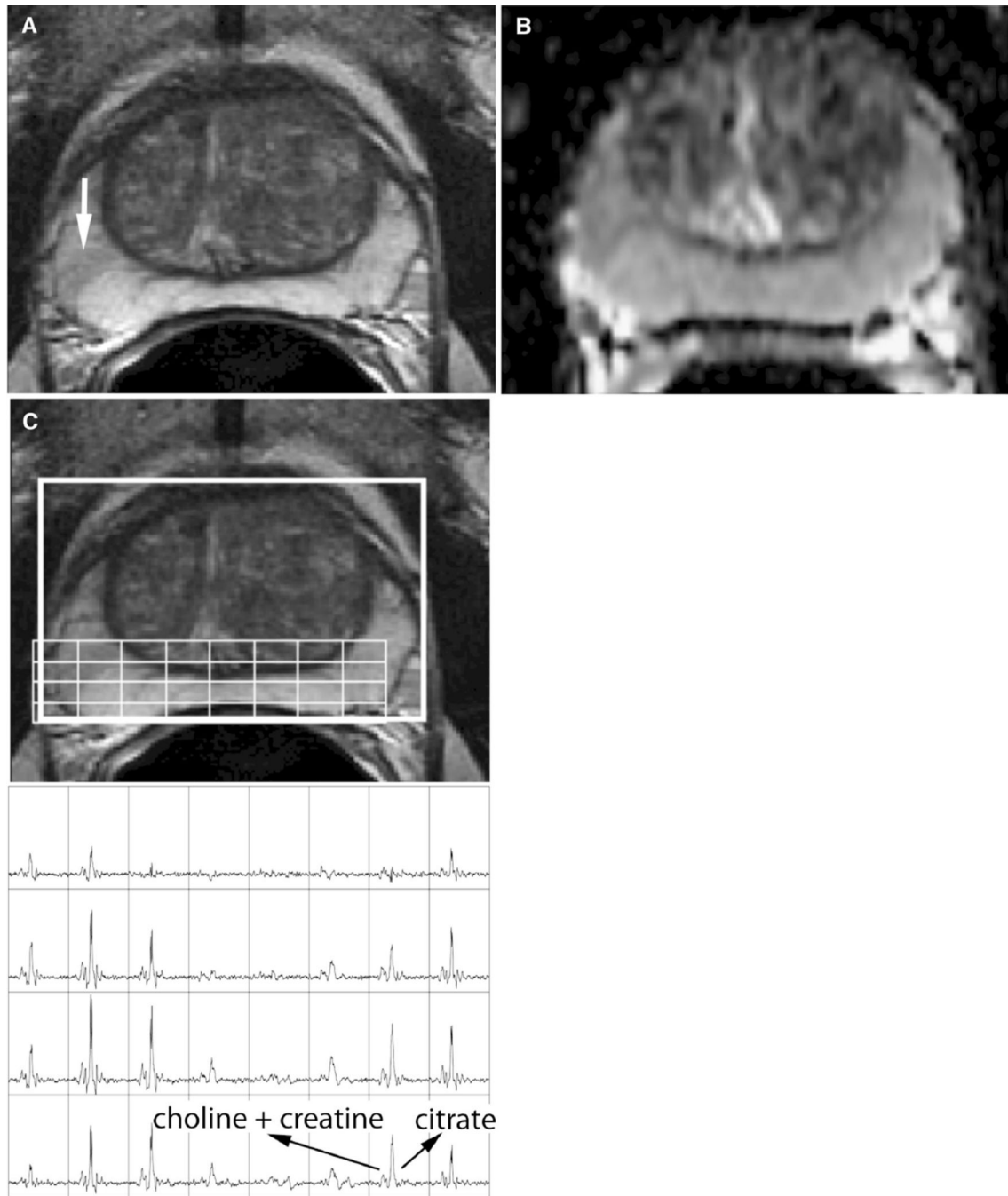
**Figure 1.**
A 60-year-old man with Gleason 3 + 3 prostate cancer, clinical stage T1c, PSA of 8.4 ng/mL. Follow-up transrectal ultrasound-guided biopsy performed 1 year after this MRI was negative. **A** T2-weighted MRI shows a faint, wedge shaped, focus of low T2 signal in the peripheral zone of the right midgland gland (*arrow*). No corresponding abnormality was seen on **B** diffusion-weighted MRI or **C** MR spectroscopic imaging.
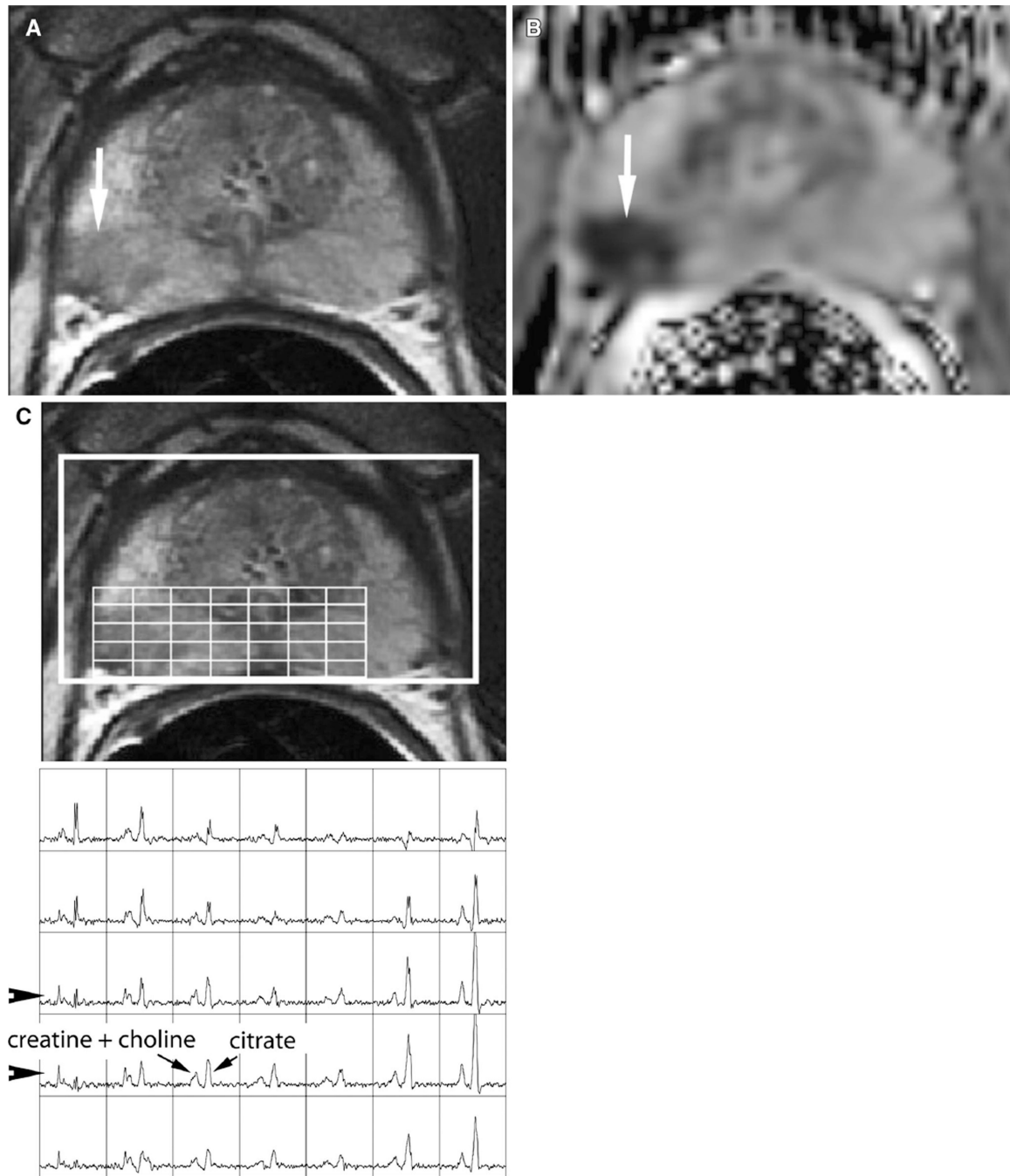
**Figure 2.**

A 68-year-old man with Gleason 3 + 3 prostate cancer, clinical stage T1c, PSA of 4.5 ng/mL. Follow-up transrectal ultrasound-guided biopsy performed 3 months after the MRI demonstrated Gleason 5 + 4 prostate cancer. **A** T2-weighted MRI shows a clear focus of low signal intensity in the peripheral zone of the right midgland gland (*arrow*). **B** Diffusion-weighted MRI shows a concordant abnormality with markedly reduced ADC (*arrow*). **C**

MR spectroscopic imaging shows abnormal metabolism characterized by high choline and low citrate peaks in the region of the T2 abnormality (*arrowheads*).

**Table 1**

Baseline population characteristics and biopsy outcome

| | |
|---|---|
| Age (years)[a] | 60.7 (45.1–74.5) |
| PSA (ng/mL)[a] | 4.7 (0.9–9.7) |
| Gleason score[b] | |
|   3 + 3 | 64 (100) |
| Clinical stage[b] | |
|   T1C | 51 (80) |
|   T2A | 12 (19) |
|   T2B | 1 (2) |
| Ethnicity[b] | |
|   Caucasian | 55 (86) |
|   African-American | 6 (9) |
|   Asian | 2 (3) |
|   Hispanic | 1 (2) |
|   Other | 2 (3) |
| Time, diagnosis to MRI (months)[a] | 4.9 (1.2–17.5) |
| Time, follow-up (months)[a] | 28.5 (2.4–116.3) |
| Gleason upgrade (n = 33)[b] | |
|   3 + 4 | 21 (64) |
|   4 + 3 | 7 (21) |
|   4 + 4 | 3 (9) |
|   4 + 5 | 1 (3) |
|   5 + 4 | 1 (3) |

*PSA* prostatic-specific antigen, *MRI* magnetic resonance imaging, *ng/mL* nanograms per milliliter

[a] Median (range)

[b] Absolute number (percentage)

**Table 2**

Imaging results

| | T2 | DWI | MRSI |
|---|---|---|---|
| Positive | 35 (54.7) | 19 (29.7) | 13 (20.3) |
| Negative | 29 (45.3) | 45 (70.3) | 51 (79.7) |

| | T2 only | MRSI only | T2 + DWI | T2 + MRSI | DWI + MRSI | All positive |
|---|---|---|---|---|---|---|
| All negative | | | | | | |
| 25 (39.1) | 19 (29.7) | 3 (4.7) | 1 (1.6) | 3 (4.7) | 1 (1.6) | 12 (18.8) |

Numbers in parenthesis are percentages

*T2* T2-weighted magnetic resonance imaging, *DWI* diffusion-weighted magnetic resonance imaging, *MRSI* magnetic resonance spectroscopic imaging

**Table 3**

Association between magnetic resonance imaging and biopsy results

| Positive MR sequences | | Biopsy upgrade | |
|---|---|---|---|
| | | No | Yes |
| 0 | | 18 (72.0) | 7 (28.0) |
| 1 | | 9 (40.9) | 13 (58.1) |
| 2 | | 2 (40.0) | 3 (60.0) |
| 3 | | 2 (16.7) | 10 (83.3) |
| | HR | *P* | 95% CI |
| | 2.49 | <0.001 | 1.72–3.62 |
| Univariate analyses | | | |
| T2 | 3.1 | <0.001 | 1.8–5.2 |
| ADC | 5.2 | <0.001 | 2.8–9.9 |
| MRSI | 2.3 | 0.01 | 1.2–4.2 |
| Multivariate analysis | | | |
| T2 | 2.5 | 0.003 | 1.4–4.5 |
| ADC | 2.8 | 0.003 | 1.1–6.7 |
| MRSI | 1.2 | 0.59 | 0.6–2.7 |

Numbers in parenthesis are percentages

*MR* magnetic resonance, *HR* hazard ratio, *P* P value, *CI* confidence interval, *T2* T2-weighted magnetic resonance imaging, *DWI* diffusion-weighted magnetic resonance imaging, *MRSI* magnetic resonance spectroscopic imaging